Received 23 November 2021; accepted 4 January 2022. Date of publication 11 January 2022; date of current version 16 February 2022.
The review of this article was arranged by Editor M.-D. Ker.

Digital Object Identifier 10.1109/JEDS.2022.3141756

Impacts of Pulsing Schemes on the Endurance of Ferroelectric Metal–Ferroelectric–Insulator–Semiconductor Capacitors

CHENG-HUNG WU[1], NICOLO' RONCHI[2], KUAN-CHI WANG[1], YU-YUN WANG[1], SEAN MCMITCHELL[2], KAUSTUV BANERJEE[2], GEERT VAN DEN BOSCH[2], JAN VAN HOUDT[2] (Fellow, IEEE), AND TIAN-LI WU[1] (Member, IEEE)

1 International College of Semiconductor Technology, National Yang Ming Chiao Tung University, Hsinchu 30010, Taiwan
2 imec, 3001 Leuven, Belgium

CORRESPONDING AUTHOR: T.-L. WU (e-mail: tlwu@nycu.edu.tw)

This work was supported in part by the "Center for the Semiconductor Technology Research" from The Featured Areas Research Center Program within the framework of the Higher Education Sprout Project by the Ministry of Education (MOE) in Taiwan; in part by the Ministry of Science and Technology, Taiwan, under Grant MOST 110-2634-F-009-027 and Grant MOST 110-2622-8-009-018-SB; and in part by the Young Scholar Fellowship Program under Grant MOST 110-2636-E-009-023.

ABSTRACT In this work, the impacts of various pulsing schemes on endurance are comprehensively investigated. Trapezoidal and triangular waveforms are considered in endurance cycling tests. For endurance cycling with the trapezoidal waveforms, different rising time (T_r)/falling time (T_f), e.g., 0.05–5 μs, with a fixed pulse width (T_{width}) and different pulse width (T_{width}), i.e., 0-10 μs, with fixed rising time (T_r)/falling time (T_f) are used. As for the endurance cycling with the triangular waveforms, the frequencies are ranged from 1 kHz to 1 MHz. The results indicate that a shorter rising time (T_r)/falling time (T_f) results in a completely different endurance characteristic, and a longer T_{width} leads to an earlier breakdown. Furthermore, the higher frequency of the triangular waveform results in a larger remnant polarization (2Pr) after endurance cycling. Overall, the endurance is highly dependent on the pulsing schemes, suggesting that a standardized methodology for the endurance evaluation is necessary for fair benchmarks and qualification of the ferroelectric-based technologies.

INDEX TERMS Ferroelectrics, endurance.

I. INTRODUCTION

HfO_2-based ferroelectric devices that are compatible with complementary metal–oxide–semiconductor (CMOS) technology are promising for memory, logic, and neuromorphic applications. Specifically, regarding to memory applications, such devices have a lower operation voltage and higher speed compared with other technologies [1]–[2]. In addition to superior performance, the endurance is regarded as the most critical reliability issue [3]–[13], which can be related to the re-distribution/generation of defects (most likely oxygen vacancy) [3]–[4], [11]–[12]. Although HfO_2-based ferroelectric devices with high endurance have been developed [2], [5], the pulsing schemes for evaluating are inconsistent. In this work, the endurance cycling tests with different pulsing schemes, including the trapezoidal waveforms with varying rising time (T_r)/falling time (T_f) and pulse width (T_{width}) and the triangular waveforms with different frequencies, are used to understand the impacts of the pulsing scheme on the endurance.

II. DEVICE STRUCTURE AND EXPERIMENTAL DETAILS

Si-doped HfO_2 ferroelectric metal–ferroelectric–insulator–semiconductor (MFIS) capacitors are used as the testing examples. **Fig. 1** illustrates the Si-doped HfO_2 ferroelectric capacitor and the transmission electron microscopy (TEM) image of the devices, fabricated on 300-mm p-type Si wafers.

This work is licensed under a Creative Commons Attribution 4.0 License. For more information, see https://creativecommons.org/licenses/by/4.0/

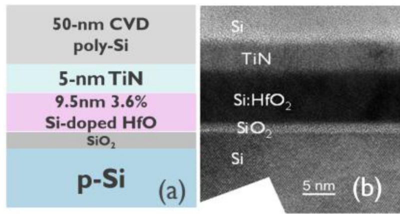

FIGURE 1. Cross section and transmission electron microscopy (TEM) image of a device used in this study.

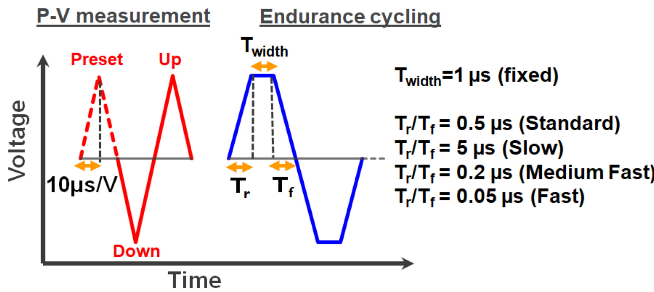

FIGURE 2. Measurement sequences in the cycling tests.

The capacitors used a 9.5-nm poly-Si/TiN/HfO_2-based ferroelectric stack with Si doping (3.6%) on the Si substrate. After the surface clean, 1nm SiO_2 interfacial layer (IL) is formed by immersing the samples in H_2O_2 solution. The ferroelectric layer was deposited by atomic layer deposition (ALD) with Si dopants. Subsequently, 5-nm TiN and 50-nm poly-Si were deposited by ALD and chemical vapor deposition, respectively. To crystallize the ferroelectric layer, a post-metallization annealing was performed in N_2 ambient for 30 s at 1000°C. The device measurements were conducted using the Keysight B1530 Waveform Generator/Fast Measurement Unit (WGFMU), which has often been used in the previous studies [14]–[16]. Three devices were measured for each condition, and the consistent results can be obtained. Therefore, one represented characteristic for each testing condition is shown for the following discussions.

III. RESULTS AND DISCUSSION

Trapezoidal waveform for the endurance cycling.

A. IMPACTS OF T_R/T_F ON ENDURANCE

A triangular waveform is used to characterize the P-V characteristics with a fixed T_r/T_f of 10 μs/V. A trapezoidal waveform is used for the endurance cycling tests. To understand the impact of T_r/T_f on the endurance reliability, four T_r/T_f conditions—from 5 μs (slow) to 0.05 μs (fast)—are used with a fixed T_{width} (**Fig. 2**). A T_r/T_f of 0.5 μs is used as the standard during the endurance cycling. The P-V characteristics under a ±4V bias with varying T_r/T_f indicate that the endurance characteristics are dependent on the T_r/T_f (**Fig. 3(a)**). Note that the device is broken after 10^3 cycles under a T_r/T_f of 0.05 μs (fast). **Fig. 3** shows the 2Pr extractions with respect to the T_r/T_f and bias voltages and the exact

TABLE 1. Summary of the 2Pr value under various T_r/T_f and bias voltage conditions.

	3V			
T_r/T_f (μs)	0.05	0.2	0.5	5
2Pr (μC/cm^2)	15.36	2.70	1.87	2.44
Max. cycling number	10^6	10^6	10^6	10^6
	4V			
T_r/T_f (μs)	0.05	0.2	0.5	5
2Pr (μC/cm^2)	22.19	14.79	11.72	12.01
Max. cycling number	10^3	10^6	10^6	10^6

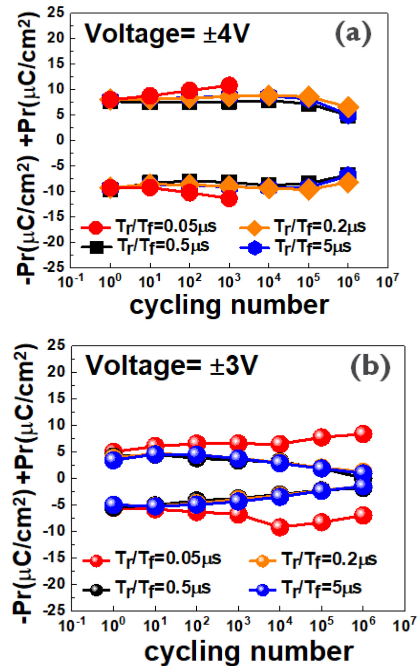

FIGURE 3. Trends of remnant polarization (2Pr) under various T_r/T_f and bias voltage conditions.

values are summarized in Table 1. In the case of the device under ±3V cycling (**Fig. 3(b)**), we can clearly observe that the device cycled with a T_r/T_f of 0.05 μs shows the completely different characteristics compared to the other cases, i.e., a slight wake-up and a larger 2Pr. Furthermore, in the case of the devices under ±4V cycling, the device cycled with a T_r/T_f of 0.05 μs shows an earlier breakdown after 10^3 cycles compared with the other cases. Last, the device tested with a T_r/T_f of 0.2 μs exhibits a slightly larger 2Pr at 10^6 cycles. Therefore, the results demonstrate that different T_r/T_f of the trapezoidal waveform used for cycling can affect the final endurance characteristics. A higher T_r/T_f indicates a longer cumulative endurance testing time. For example, the total endurance testing time to 10^6 cycles under a T_r/T_f of 0.05 and 5 μs is 2.2 and 22 s, respectively. However, a shorter cumulative endurance testing time results in a larger 2Pr at the end of testing—or even, an earlier breakdown (**Fig. 3(a)**). In order to further understand the impact of

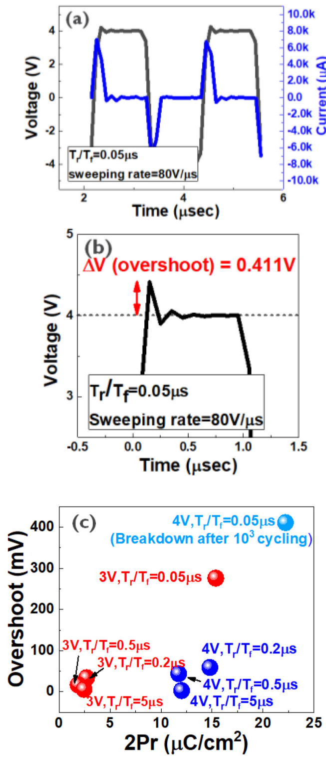

FIGURE 4. Example of record voltage and current in the case of $T_r/T_f = 0.05$ μs (a), overshoot in the case of $T_r/T_f = 0.05$ μs (b), and the summary of the voltage overshoot versus 2Pr (c).

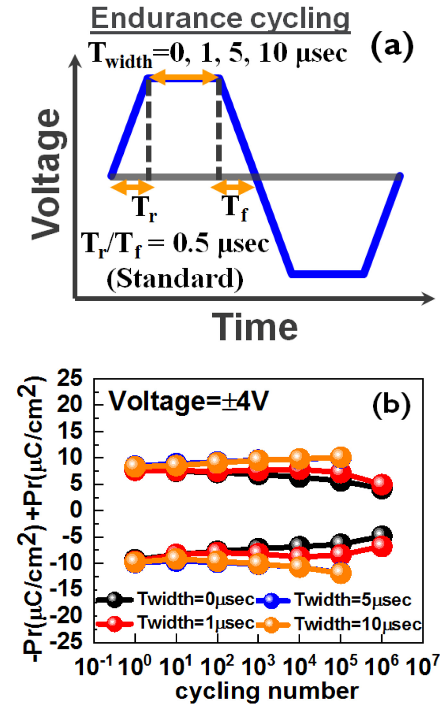

FIGURE 5. (a) Schematic of the cycling waveform under differing T_{width}. (b) Trend of remnant polarization (2Pr). Note that T_r/T_f of 0.5 μs is selected as a standard to minimize the effects of the voltage overshoot.

T_r/T_f, **Fig. 4(a)** shows the recorded voltage and switching current during the tests. The device tested with a lower T_r/T_f (i.e., a high sweeping rate (dV/dt)), has a large total current (**Fig. 4(a)**) and an obvious voltage overshoot (**Fig. 4(b)**).

The total current consists of the 1) polarization switching-induced current, 2) displacement current due to dV/dt, and 3) conduction current of the material (I_C) as shown below [17]:

$$I(t) = A \times \frac{dP(t)}{dt} + C \times \frac{dV(t)}{dt} + I_C,$$

where A is the area, t is the time, $P(t)$ is the ferroelectric polarization, C is the parallel plate capacitance, and $V(t)$ is the applied voltage. Therefore, the high sweeping rate (dV/dt) results in a large $C \times \frac{dV(t)}{dt}$, which further contributes to the total current during the polarization switching (**Fig. 4(a)**). Moreover, a voltage overshoot ($\Delta V = 0.411V$) occurred under a T_r/T_f of 0.05 μs is clearly observed (**Fig. 4(b)**). **Fig. 4(c)** shows the summary of the voltage overshoot during the cycling test with respect to the 2Pr. This indicates that the difference in endurance under a T_r/T_f of 0.05 μs is most likely due to the voltage overshoot. When the voltage overshoot is below 100mV, it results in a limited impact on the 2Pr. On the other hand, the larger voltage overshoot has a positive correlation with the larger 2Pr at ±3V cycling and with the earlier breakdown at ±4V cycling. Therefore, the completely different endurance performance with a $T_r/T_f = 0.05$μs can be most probably due to the larger voltage overshoot. The larger voltage overshoot can result in a larger electric field applied to the FE layer. This issue can both influence the reorientation of polarization and defect generation and distribution, resulting in the different wake-up and degradation [4], [12]. The similar overshoot issue is also observed in the recent literature [18], showing ~10% voltage overshoot with reported gate voltage pulsing waveform with $T_r/T_f = 10$ns.

B. IMPACTS OF T_{WIDTH} ON ENDURANCE

During the cycling endurance tests with the trapezoidal waveform, T_{width} can be varied. **Fig. 5(a)** shows a schematic of the trapezoidal waveform in the cycling endurance tests under differing T_{width} (0, 1, 5, and 10 μs) and a fixed T_r/T_f of 0.5 μs. The 2Pr extraction vs. cycling number with different T_{width} is shown in **Fig. 5(b)**, observing that T_{width} has the impact on the endurance characteristics. For example, 2Pr is slightly large once the T_{width} is increased from 0μs to 1μs . When T_{width} is increased to 5 or 10 μs, a breakdown is occurred after 10^5 cycles. A longer T_{width} can 1) improve the wake-up efficiency [19]–[23], which might be related to the defect redistribution [3]–[4], and 2) result in time-dependent dielectric breakdown [24] that can cause an earlier cycle-to-breakdown due to a longer stress time.

Triangular Waveform in Cycling Endurance Tests: In addition to the trapezoidal waveform, a triangular pulsing scheme is one of the most common waveforms to evaluate the

TABLE 2. Comparison of the pulsing schemes in the recent reported ferroelectric-based capacitors.

		[5]	[6]	[7]	[8]	[13]	[14]	[15]	This work	
Structure		MFIS	SFS	MFS	MFS	MFM	MFM	MFM	MFIS	
Substrate		p-Si	p-Si	SiGe	Ge	TiN as the bottom electrode	Pt	TiN or Ru	p-Si	
Film (thickness)		$Al:HfO_2$ (15nm)	$Al:HfO_2$ (8nm)	HZO (10nm)	$Y:HfO_2$ (5nm)	$Si:HfO_2$ (10nm)	$Y:HfO_2$ (15nm)	HZO (10nm)	$Si:HfO_2$ (9.5nm)	
P-V measurement	Waveform	Triangular	Triangular			Triangular	Triangular		Triangular	
	Time parameter	Freq: 1kHz	Sweeping rate =10μs/V		Freq: 10kHz	Freq: 1k Hz	Freq: 1k Hz		Sweeping rate=10μs/V	
Endurance Cycling	Waveform	Only mentioned bipolar	Trapezoidal	Only mentioned bipolar	Triangular	Only mentioned bipolar		Only mentioned bipolar	Trapezoidal	Triangular
	Frequency (kHz)	10		1/10/100	100	5/10/50/100	10/20/30/50/70/100	1M		1/100/1000
	$T_r/T_f/T_{width}$		T_r/T_f=0.5μs T_{width}=1μs						T_r/T_f= 0.2/0.5/5μs T_{width}=1μs	T_r/T_f=250/2.5/0.25μs
	T_{period}									T_{period}=1m/10μ/1μs
Max. endurance cycle		10^9	10^5	10^9	10^8	10^9	~10^8	~10^{10}/~10^{11}	10^3~10^6	10^6
Voltage bias		±6V	±3/3.5/4/4.5V	±4V	±1.5V	±2/3.5V	±3V	±3/3.5V	±3/4V	±3/4V

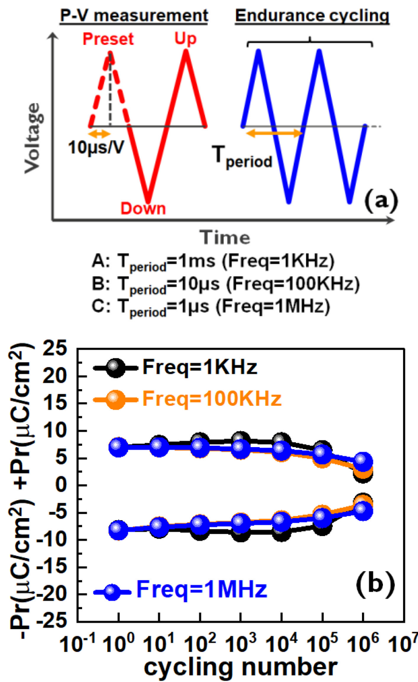

FIGURE 6. (a) Measurement sequences of endurance evaluation with a triangular waveform. (b) Summary of remnant polarization (2Pr) trends. Note that the impact of the voltage overshoot is limited because the voltage is lower than 30 mV in the cycling endurance tests with the triangular waveform for all of the varied frequencies.

endurance reliability as well. **Fig. 6(a)** shows the measurement sequence of endurance evaluation with a triangular waveform. Three different frequencies from 1 kHz to 1 MHz are used. **Fig. 6(b)** shows that different frequencies during the cycling test result in the different endurance characteristics. A higher frequency results in a smaller 2Pr before 10^5 cycles, which is consistent with the reported literature explained by the concept of switchable region [13]. On the other hand, a higher frequency also results in a slight degradation in 2Pr at 10^6 cycles, most probably related to the limited dipole switching [9]–[11] that can suppress the generation of oxygen vacancies [11]. A higher frequency can also limit the dipole switching due to a shorter switching time since the reported dipole switching time is in the range from 0.2μsec to 2msec [19] depending on the effective bias and material properties under the nucleation limited switching (NLS) model [19]–[23]. Therefore, the ferroelectric dipoles might be unable to respond, leading to a minor 2Pr degradation at the cycling number of 10^6. **Fig. 7** shows the benchmark of the endurance for the different pulsing schemes used in this work, which, to the best of our knowledge, has never been reported before. We can clearly observe that the endurance reliability is highly dependent on the pulsing schemes. **Table 2** summarizes the recent reported cycling characteristics in ferroelectric-based capacitors, showing that there is no consistent pulsing scheme to evaluate the cycling characteristics and some of the pulsing details are not disclosed [5]–[8], [13]–[15]. Therefore, the benchmarking comparison within different works can be misleading due to the inconsistent pulsing schemes. A consistent methodology for evaluating endurance reliability is necessary for the assessment and qualification of ferroelectric-based technologies.

IV. CONCLUSION

In this work, to the best of our knowledge, the effects of the pulsing scheme on the endurance are comprehensively studied for the first time in Si-doped HfO_2 MFIS capacitors

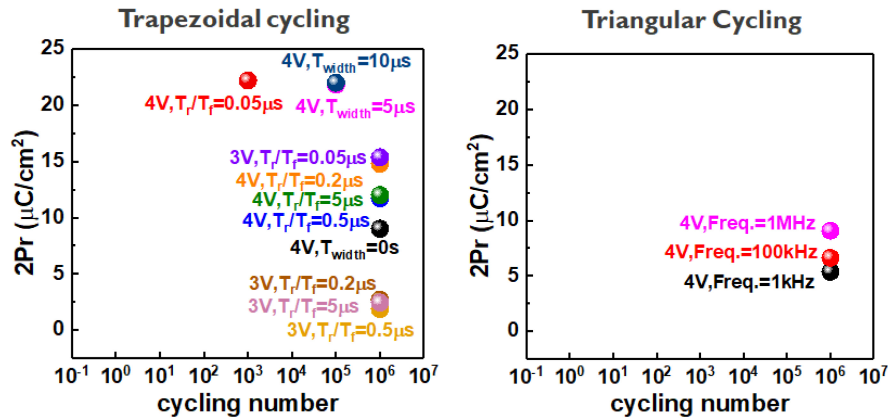

FIGURE 7. 2Pr characteristics versus the pulsing schemes.

by considering the endurance cycling tests with 1) different T_r/T_f values with a fixed T_{width} in the trapezoidal waveform, 2) different T_{width} values with a fixed T_r/T_f in the trapezoidal waveform, and 3) different frequencies in the triangular waveform. First, it is the first time to report that the endurance cycling tests with a shorter T_r/T_f results in the completely different 2Pr characteristics, leading to a larger 2Pr in the case of $\pm$3V and an earlier breakdown in the case of $\pm$4V, which is most probably due to the overshoot. Since the devices are identical in this study, the endurance result can be influenced by the voltage overshoot, which is independent of the device characteristics. Secondly, a longer T_{width} during the trapezoidal waveform can 1) increase 2Pr (in the case of $T_{width} = 1$ μs) and 2) result in an earlier breakdown (in the case of $T_{width} = 5$ and 10 μs). Finally, considering the endurance cycling test with the triangular waveform, high frequencies can increase the 2Pr at 10^6 cycles. In summary, we demonstrate that the endurance is sensitive to the pulsing schemes, which can lead to misleading evaluation and comparison among the results found in the literature. A standardized methodology to test the endurance reliability is needed for the development, benchmark, and qualification of the ferroelectric-based technologies. Using the consistent pulsing schemes to have a fair endurance evaluation and to unify the degradation mechanisms can be the future work to advance the ferroelectric-based technologies. Similar studies for the other ferroelectric-based technologies, such as metal–ferroelectric–metal capacitors, ferroelectric field-effect transistors, and negative capacitance field-effect transistors, and the neuromorphic operations, can be the future works as well since the understanding of the impacts of the pulsing schemes on the performance and reliability in these technologies have not been discussed in details yet.

REFERENCES

[1] T. S. Böscke, J. Müller, D. Bräuhaus, U. Schröder, and U. Böttger, "Ferroelectricity in hafnium oxide thin films," *Appl. Phys. Lett.*, vol. 99, no. 10, Sep. 2011, Art. no. 102903, doi: 10.1063/1.3634052.

[2] J. Müller *et al.*, "Ferroelectric hafnium oxide: A CMOS-compatible and highly scalable approach to future ferroelectric memories," in *IEDM Tech. Dig.*, Washington, DC, USA, Dec. 2013, pp. 1–4, doi: 10.1109/IEDM.2013.6724605.

[3] A. Chouprik *et al.*, "Wake-up in a Hf0.5Zr0.5O2 film: A cycle-by-cycle emergence of the remnant polarization via the domain depinning and the vanishing of the anomalous polarization switching," *ACS Appl. Electron. Mater.*, vol. 1, no. 3, pp. 275–287, 2019, doi: 10.1021/acsaelm.8b00046.

[4] M. Peši'c *et al.*, "Physical mechanisms behind the field-cycling behavior of HfO2-based ferroelectric capacitors," *Adv. Funct. Mater.*, vol. 26, no. 25, pp. 4601–4612, 2016, doi: 10.1002/adfm.201600590.

[5] S. Oh, J. Song, I. K. Yoo, and H. Hwang, "Improved Endurance of HfO2-based metal-ferroelectric-insulator-silicon structure by high-pressure hydrogen annealing," *IEEE Electron Device Lett.*, vol. 40, no. 7, pp. 1092–1095, Jul. 2019, doi: 10.1109/LED.2019.2914700.

[6] K. Florent *et al.*, "Reliability study of ferroelectric Al: HfO2 thin films for DRAM and NAND applications," *IEEE Trans. Electron Devices*, vol. 64, no. 10, pp. 4091–4098, Oct. 2017, doi: 10.1109/TED.2017.2742549.

[7] K.-Y. Chen, Y.-H. Huang, R.-W. Kao, Y.-X. Lin, and Y.-H. Wu, "Dependence of reliability of ferroelectric HfZrOx on epitaxial SiGe film with various Ge content," in *Proc. IEEE Symp. VLSI Technol.*, Honolulu, HI, USA, 2018, pp. 119–120, doi: 10.1109/VLSIT.2018.8510643.

[8] X. Tian *et al.*, "Sub-nm EOT ferroelectric HfO2 on p+Ge with highly reliable field cycling properties," in *Proc. IEEE Int. Electron Devices Meeting (IEDM)*, San Francisco, CA, USA, 2017, pp. 1–4, doi: 10.1109/IEDM.2017.8268508.

[9] D. Zhou *et al.*, "Wake-up effects in Si-doped hafnium oxide ferroelectric thin films," *Appl. Phys. Lett.*, vol. 103, no. 19, Nov. 2013, Art. no. 192904, doi: 10.1063/1.4829064.

[10] R. Cao *et al.*, "Improvement of endurance in HZO-based ferroelectric capacitor using Ru electrode," *IEEE Electron Device Lett.*, vol. 40, no. 11, pp. 1744–1747, Nov. 2019, doi: 10.1109/LED.2019.2944960.

[11] S. Starschich, S. Menzel, and U. Böttger, "Pulse wake-up and breakdown investigation of ferroelectric yttrium doped HfO2," *Appl. Phys. Lett.*, vol. 121, no. 15, Apr. 2017, Art. no. 154102, doi: 10.1063/1.4981893.

[12] U. Celano *et al.*, "Probing the evolution of electrically active defects in doped ferroelectric HfO2 during wake-up and fatigue," in *Proc. IEEE Symp. VLSI Technol.*, Honolulu, HI, USA, 2020, pp. 1–2, doi: 10.1109/VLSITechnology18217.2020.9265098.

[13] S. Li, D. Zhou, Z. Shi, M. Hoffmann, T. Mikolajick, and U. Schroeder, "Involvement of unsaturated switching in the endurance cycling of Si-doped HfO2 ferroelectric thin films in advanced electronic materials," *Adv. Electron. Mater.*, vol. 6, no. 8, 2020, Art. no. 2000264, doi: 10.1002/aelm.202000264.

[14] T. Francois *et al.*, "Ferroelectric HfO2 for memory applications: Impact of si doping technique and bias pulse engineering on switching performance," in *Proc. IEEE 11th Int. Memory Workshop (IMW)*, Monterey, CA, USA, 2019, pp. 1–4, doi: 10.1109/IMW.2019.8739664.

[15] K. Lee, J. Bae, S. Kim, J. Lee, B. Park, and D. Kwon, "Ferroelectric-gate field-effect transistor memory with recessed channel," *IEEE Electron Device Lett.*, vol. 41, no. 8, pp. 1201–1204, Aug. 2020, doi: 10.1109/LED.2020.3001129.

[16] K. Lee, S. Kim, J. Lee, D. Kwon, and B. Park, "Analysis on reverse drain-induced barrier lowering and negative differential resistance of ferroelectric-gate field-effect transistor memory," *IEEE Electron Device Lett.*, vol. 41, no. 8, pp. 1197–1200, Aug. 2020, doi: 10.1109/LED.2020.3000766.

[17] B. Dickens, E. Balizer, A. S. DeReggi, and S. C. Roth, "Hysteresis measurement of remanent polarization and coercive field in polymers," *J. Appl. Phys.*, vol. 72, no. 9, pp. 4258–4264, 1992, doi: 10.1063/1.352213.

[18] A. J. Tan *et al.*, "Ferroelectric HfO2 memory transistors with high-κ interfacial layer and write endurance exceeding 1010 cycles," *IEEE Electron Device Lett.*, vol. 42, no. 7, pp. 994–997, Jul. 2021, doi: 10.1109/LED.2021.3083219.

[19] P. Pandey, W. S. Hwang, K. R. Udayakumar, T. S. Moise, and A. C. Seabaugh, "Programming-pulse dependence of ferroelectric partial polarization: Insights from a comparative study of PZT and HZO capacitors," *IEEE Trans. Electron Devices*, vol. 67, no. 10, pp. 4482–4487, Oct. 2020, doi: 10.1109/TED.2020.3015794.

[20] H. Mulaosmanovic *et al.*, "Impact of read operation on the performance of HfO2-based ferroelectric FETs," *IEEE Electron Device Lett.*, vol. 41, no. 9, pp. 1420–1423, Sep. 2020, doi: 10.1109/LED.2020.3007220.

[21] C. Alessandri, P. Pandey, A. Abusleme, and A. Seabaugh, "Switching dynamics of ferroelectric Zr-doped HfO2," *IEEE Electron Device Lett.*, vol. 39, no. 11, pp. 1780–1783, Nov. 2018, doi: 10.1109/LED.2018.2872124.

[22] S. Mueller, S. R. Summerfelt, J. Muller, U. Schroeder, and T. Mikolajick, "Ten-nanometer ferroelectric Si: HfO2 films for next-generation FRAM capacitors," *IEEE Electron Device Lett.*, vol. 33, no. 9, pp. 1300–1302, Sep. 2012, doi: 10.1109/LED.2012.2204856.

[23] T. Y. Lee *et al.*, "Ferroelectric polarization-switching dynamics and wake-up effect in Si-doped HfO 2," *ACS Appl. Mater. Interfaces*, vol. 11, no. 3, pp. 3142–3149, 2019, doi: 10.1021/acsami.8b11681.

[24] Y.-H. Chen, C.-J. Su, T.-H. Yang, C. Hu, and T.-L. Wu, "Improved TDDB reliability and interface states in 5-nm Hf0.5Zr0.5O2 ferroelectric technologies using nh3 plasma and microwave annealing," *IEEE Trans. Electron Devices*, vol. 67, no. 4, pp. 1581–1585, Apr. 2020, doi: 10.1109/TED.2020.2973652.